

Modelling biochemical processes in orchards at leaf- and canopy-level using hyperspectral data

S. Delalieux^a, P. Kempeneers^b, J.A.N.van Aardt^c, S. De Backer^d, P. J. Zarco-Tejada^e, G. Sepulcre-Cantó^e, R. Sagardoy^f, F. Morales Iribas^f, P. Scheunders^d, and P. Coppin^a

^aKatholieke Universiteit Leuven, Celestijnenlaan 200E, B-3001 Heverlee, Belgium

^bFlemish Institute for Technological Research (VITO), Boeretang 200, B-2400 Mol, Belgium

^cCSIR - NRE Ecosystems Earth Observations, P.O. Box 395, Pretoria 0001, South Africa

^dUniversity of Antwerpen, Groenenborgerlaan 171, B-2020 Antwerpen, Belgium

^eInstituto de Agricultura Sostenible (IAS-CSIC), Córdoba, Spain

^fEstación Experimental Aula Dei (EEAD-CSIC), Zaragoza, Spain

Abstract:

This research was conducted to evaluate the potential and limitations of hyperspectral remote sensing to detect iron deficiency in capital-intensive multi-annual crop systems, e.g. peach orchards. The noted deficiency can be regarded as a proxy for deviations from optimal plant functioning, while detection of such deviations is in turn of significant importance to monitoring and modelling efforts of orchards as production systems. Hyperspectral leaf, canopy, and airborne reflectance measurements were acquired in a peach (*Prunus persica* L.) orchard in Zaragoza, Spain. Leaf- and canopy-level data were collected with a handheld spectroradiometer (ASD, Inc.), while the AHS-160 hyperspectral sensor provided airborne data. Blocks of trees were treated with different amount of iron chelates (Sequestrene) which created a dynamic range of chlorophyll concentration as measured in leaves.

Hyperspectral measurements at leaf-level were carried out to characterize the physiological aspects of nutrient stress, as opposed to the evaluation of plant nutrient status at the complete plant-level. Stress-induced physiological changes make stress detection at the leaf-level possible at an early stage of sub-optimal photosynthetic functioning. Airborne imagery, however, is difficult to interpret due to altering illumination angles, BRDF effects, and intervening atmospheric light interactions resulting in an alteration of the vegetative reflectance spectrum. Although many studies have implemented hyperspectral analysis of nutrient status at large scales, this research field is still in its infancy phase, since the link between airborne- and leaf-level measurements is lacking. This inevitably makes the physiological interpretation of existing hyperspectral research more complex. The multi-level (leaf, canopy, and airborne) approach presented here enabled the assessment of vegetation indices and their relationship with pigment concentration at each monitoring level. Pertinent classical chlorophyll-related vegetation indices were tested and new indices were extracted from the spectral profiles by means of band reduction techniques and narrow-waveband rationing, which involved all possible 2-band combinations. Robustness was evaluated by studying the index performance for datasets of increasing complexity, from leaf- to canopy- and airborne-level. Physiological interpretations extracted from leaf-level experiments were extrapolated to canopy- and airborne level.

The measured spectra and estimated biochemical parameters were related via inversion of a linked directional homogeneous canopy reflectance model (ACRM) and the PROSPECT leaf model. Numerical model inversion was conducted by minimizing the difference between the measured reflectance samples and modelled reflectance values. An improved optimization method is presented. Results are compared with a simple linear regression analysis, linking chlorophyll to the reflectance measured at the leaf level and at the Top of Canopy (TOC), while optimal band regions and bandwidths also were analyzed.

Keywords: hyperspectral data extraction, vegetation indices, vegetation stress detection, model inversion, canopy reflectance model

1. Introduction

The use of non-destructive methods for the detection of vegetation stress holds great promise for optimization of the management of commercially important agricultural crops. Timely and efficient agricultural management of orchards can improve yield and fruit quality (Cordeiro *et al.*, 1995, Tagliavini and Rombola, 2001). The fact that the amount of reflected light depends on a number of leaf-related factors, such as external morphology, internal structure, and internal distribution of biochemical components, etc., makes it possible for hyperspectral remote sensing to detect deviations from optimally functioning plant systems. I.e., stress-induced physiological changes will affect leaf biochemical constituents such as chlorophyll concentration (C_{ab}) and water content. These constituents in turn can be estimated from airborne image acquisition, thereby making stress detection at the leaf-level possible at an early stage of sub-optimal photosynthetic functioning. Even though hyperspectral data can be beneficial to various applications, data volume and dimensionality cause both technical (storage capacity, CPU time for processing, data transfer, etc.) and statistical problems. Hence, the development and optimization of band reduction techniques and vegetation indices using only a limited amount of data are of utmost importance. In this study we attempted to generate novel, robust indices that enable effective detection and quantification of anomalies in the “normal” plant production process at leaf, canopy and airborne level.

Carter (1993) determined the wavelengths at which leaf reflectance was generally most responsive to stress. He found that due to decreased absorption by pigments, reflectance at visible wavelengths increased consistently with stressed leaves for eight stress agents and among six vascular plant species. Visible reflectance seemed to be most sensitive to stress in the 535-640 nm and 685-700 nm wavelength ranges. Infrared reflectance was comparatively unresponsive to stress, but increased at 1400-2500 nm with severe leaf dehydration and the accompanying decreased absorption by water. Similar results were obtained in other studies investigating plant stresses (Lorenzen and Jensen, 1989, Penuelas *et al.*, 1994, Filella *et al.*, 1995, Gamon *et al.*, 1995). The induced iron stress in this study was chosen to emphasize those findings, because iron catalyzes the production of chlorophyll, which is the critical component in the photosynthetic cycle, and differences in reflectance due to changes in chlorophyll concentration are expressed in the visible region of the spectrum. Iron is indispensable to the plant as a component of enzymes and light energy transferring compounds central to photosynthesis, and is moreover involved in the reduction of nitrates and sulphates.

For that reason, the focus of the second part of this paper lies in the retrieval of chlorophyll content from airborne imagery and *in situ* measured reflectance spectra. Different techniques were used to retrieve chlorophyll from both leaf reflectance spectra measured in the field and canopy reflectance from airborne hyperspectral data. A simple linear regression analysis confirmed the importance of the green peak and red-edge for chlorophyll retrieval (Carter, 1994, Gitelson and Merzlyak, 1996). We further analyzed specific wavelengths for a successful estimation of C_{ab} . However, regression techniques require training data and the predictive algorithm is not generally applicable (Grossman, 1996). The selected bands depend on the dataset at hand, influenced by species, canopy structure and viewing geometry.

A more general approach is to implement radiative transfer models in order to explain the measured reflectance signatures of canopies. When inverted, they also allow the estimation of leaf biochemistry from remote sensing data. Most successful applications of radiative transfer models for this purpose involve closed crop canopies (Jacquemoud *et al.*, 1995, 2000). A major issue of open canopies such as the peach orchard in this study is the relative large contribution of soil background and shadows which dominate the bi-directional reflectance (BRDF) signature (Zarco-Tejada *et al.*, 2004). Nevertheless, good correspondence was found between estimated C_{ab} from airborne hyperspectral data and *in situ* measurements, with both linear regression and model inversion. An improved methodology for model inversion is proposed in this paper. The main objectives thus were to determine (i) whether logistic regression and associated index development can be used to differentiate between various iron treatments at the leaf-, canopy-, and airborne level and (ii) whether chlorophyll content can be accurately estimated using leaf-, canopy-, and airborne level spectra, through implementation of standard regression and model inversion techniques.

2. Methodology

2.1. Iron deficiency: Logistic regression based on vegetation indices

Most of the classical vegetation indices developed to detect stress in plants are based on chlorophyll (Carter, 1994, Daughtry *et al.*, 2000, Gamon *et al.*, 1992, Gitelson *et al.*, 1996, Peñuelas *et al.*, 1995, Lichtenthaler *et al.*, 1996, Penuelas *et al.*, 1994, 1995, Zarco-Tejada *et al.*, 2001) and water content (Eitel *et al.*, 2006, Pu *et al.*, 2003). Generally, these indices are expressed in (relative) difference of bands or band ratio's. However, leaf and canopy structure have a considerable impact on the efficacy of such indices, thereby making it impossible to use them at all levels (leaf, canopy, airborne). Several techniques have been introduced to increase the robustness of biochemical parameter estimation (Blackmer *et al.*, 1996, Chappelle *et al.*, 1992, Daughtry *et al.*, 2000, Kokaly and Clark, 1999). Haboudane *et al.* (2002) proposed an index that linked chlorophyll to the vegetation indexes TCARI (Transformed Chlorophyll Absorption Ratio Index) and OSAVI (Optimized Soils Adjusted Vegetation Index) (Eq. 1). It was obtained using simulated data and good results were obtained for a wide range of leaf area index values.

$$\text{Chl} = -30.605 * \ln(\text{TCARI}/\text{OSAVI}) \quad \text{Eq.1}$$

$$\text{TCARI} = 3((R_{700} - R_{670}) - 0.2(R_{700} - R_{550}))(R_{700}/R_{670}) \quad \text{Eq.2}$$

$$\text{OSAVI} = (1 + 0.16)(R_{800} - R_{670}) / (R_{800} + R_{670} + 0.16) \quad \text{Eq.3}$$

A drawback of the indices is that band locations and bandwidths vary with sensors. As a result, values are sensor dependent, requiring a calibration step. As an example, the nearest central wavelengths available in the AHS sensor are shown in Table 1.

Table 1: Suggested bands by Haboudane and available band in AHS sensor

Suggested band Haboudane	Available band AHS	Bandwidth
550nm	542nm	28nm
670nm	659nm	28nm
700nm	718nm	28nm
800nm	804nm	28nm

It should be noted that, although the TCARI/OSAVI index was tested with the available AHS wavelengths, it did not yield optimal results in our study at leaf level (*c*-index value=0.69). Hence, a standardized difference of the measured reflectance values was calculated for each possible combination of two different wavelengths (see Eq. 4) at the three measurement levels, thereby evading the environmental and structural effects on the reflectance patterns. This standardized difference was used as independent variable in a logistic regression analysis to test the discriminatory performance of the index. This approach allows for selection of an optimal standardized difference vegetation index, as well as being a tool to test existing vegetation indices. Logistic regression *c*-values above 0.8 were considered indicative of adequate discriminatory performance.

$$\text{SDVI} = \frac{\text{wavelength 2} - \text{wavelength 1}}{\text{wavelength 2} + \text{wavelength 1}} \quad \text{Eq.4}$$

2.2. Chlorophyll retrieval: Regression

Stepwise multiple linear regression (MLR) (Curran *et al.*, 1992, Martin and Aber, 1997, Wessman *et al.*, 1988) is an empirical approach which develops a predictive algorithm for chlorophyll from leaf or canopy reflectance. It estimates the statistical relationship between the chlorophyll concentration and specific reflectance bands from a training dataset. Camps-Valls *et al.* (2006) suggests a robust regression based on support vector machines that is particularly useful in cases with limited *in situ* measurements. Regression can be performed both at leaf- and canopy level. However, results seem to be inconsistent if not trained at the appropriate level. Most importantly, the predictive algorithm, trained on a specific site and crop, is not reliable for other conditions (Grossman *et al.*, 1996). The selected bands depend on the dataset at hand, influenced by species, canopy structure and viewing geometry. If properly trained, regression methods however can be very useful for a specific dataset at hand. It allows analysis of band regions and bandwidths of interest, as shown in section 3.

A linear regression was performed at leaf- and top of canopy level in this study. The chlorophyll values measured *in situ* were used as the response value in the regression analysis. The explanatory variable was the reflectance value in one (simple linear regression) or more bands (multiple regression). The optimal band was selected from the available spectrum through minimization of the residual sum of squared errors after regression. Bands were selected using multivariate statistics in the case of multiple bands, considering the best combination of two bands based on a training set.

2.3. Chlorophyll retrieval: Model inversion

Another technique to retrieve chlorophyll from reflectance data is through numerical inversion of leaf and canopy reflectance models. Inversion is usually performed with an iterative optimization method (section 2.3), though lookup tables and neural networks are also used. Foliar chlorophyll can be retrieved from leaf reflectance by inverting a leaf model such as PROSPECT (Jacquemoud *et al.*, 1996). The leaf model must be coupled with a canopy model in order to estimate biochemical parameters from canopy reflectance. We used the radiative transfer canopy model ACRM (Kuusk, 1995, 1995, 2003) for this purpose.

The numerical inversion minimizes a merit or cost function. This is typically the sum of squared differences between the measured and modelled canopy spectral reflectance in each spectral band ($i=1\dots d$) (Zarco-Tejada, 2001):

$$\Delta^2 = \sum_{i=1}^d \left(R_i - \hat{R}_i(P) \right)^2 \quad (5)$$

The modelled reflectance \hat{R} depends on the model parameters P . The optimization thus consists of finding the optimal model parameters P that minimize the merit function. Modifications of this merit function exist, for example by weighing the contributions of the individual wavelengths.

In Zarco-Tejada *et al.* (2001), the merit function is based on an optical index (R_{750}/R_{710}) that focused on a single band ratio, rather than the entire spectrum. The authors claimed superior results when a methodology consisting on minimizing a function based in a red edge optical index was used, rather than by matching all the reflectance bands in the visible and NIR, especially if reflectance signals included shadowed pixels. A different approach was followed in this study, where we filtered the modelled reflectance \hat{R} to simulate the reflectance measured by the airborne hyperspectral sensor. It is important to match the modelled spectrum to the sensor specifications, especially for sensors such as the AHS sensor, which has varying bandwidths. Figure 1 shows the modelled spectrum before and after filtering.

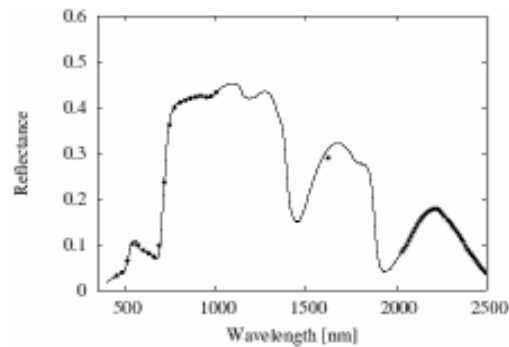


Figure 1: The modelled canopy spectrum before (solid) and after (dots) filtering according to the specifications of the AHS sensor.

Finding the minimum merit function is not straightforward. Analytic solutions are unfeasible due to the high non-linearity of the problem. Moreover, it may have multiple separated local minima. Only one of these minima represents the true global minimum of interest. Gradient descent algorithms include steepest-descent, conjugate-gradient, quasi-Newton and Levenberg-Marquardt algorithms (Moré, 1978). They have a low computational cost, but can easily be stuck at a local minimum, depending on the initialization of the parameters.

Global search methods overcome the local minimum pitfall, but have a higher computational cost. We adopted the adaptive simulated annealing (ASA Ingber) for the optimization scheme. It is a very fast implementation of the simulated annealing algorithm (Kirkpatrick, 1983) with some optimizations such as a re-annealing schedule. We compared our optimization with the conjugate direction method of Powell (Powell, 1964), included in the available inversion routines of ACRM by Nilson and Kuusk (1989).

3. Experiments

3.1. Experimental setup

The peach orchard is schematically presented in Figure 12. The plot, represented as a matrix, consists of 35 rows and 6 columns. The total number of trees is 205 instead of 210, due to five missing trees (indicated in red). Each pixel corresponds to the extracted tree canopy spectrum (gray levels represent the reflectance in red). Iron chlorosis was induced in the two rightmost columns (pixels indicated in blue). Trees were treated in groups of three as indicated. The iron chelate was applied according to the blue color code (from light to dark): 0g/tree, 60g/tree, 90g/tree, and 120g/tree. The yellow pixels represent trees that have been grafted during the previous year (2004).

3.2. Field data collection

Fresh leaves were sampled for each tree and measured with the ASD spectrometer. Leaf reflectance was measured for 716 leaves, using a leaf clip ASD assembly. Chlorophyll was measured for each leaf with a SPAD-502 Minolta Chlorophyll Meter and mean values were calculated per tree to compare with parameters obtained at the canopy level. The SPAD measurements were calibrated to obtain chlorophyll concentration, by comparing SPAD readings with concentrations derived from destructive chemical analysis in the laboratory for a subset of leaf samples. The result is shown in Figure 2. A correlation coefficient of 0.82 was obtained.

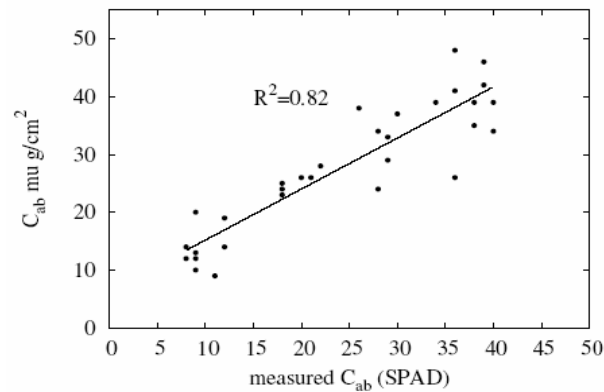


Figure 2: Calibration of the SPAD values using C_{ab} concentrations derived from chemical analysis in the laboratory.

3.3. Airborne hyperspectral data

The AHS sensor has 63 bands covering the visual and near infrared part of the spectrum (450nm-2500nm). Image data were processed to top of canopy level, using in-house developed software for atmospheric correction based on MODTRAN. The ground resolution of 2.5m was slightly larger than the crown diameter, which complicated tree identification in the image. The peach trees were planted according to the scheme in Figure 12 at a spacing of 4 meters (8/5 pixels). The hyperspectral image was scaled up using a factor of five (nearest neighbor resampling) in order to facilitate tree extraction. Any given tree therefore was covered in a region of interest (ROI) with a whole number of (sub) pixels. The sub-pixels contain exactly the same spectral information as the original pixels, since nearest neighbor resampling was used. The median reflectance of the sub-pixels in the ROI was used to obtain target canopy reflectance. An alternative was to select the pixel in the ROI with maximum normalized difference vegetation index (NDVI) or maximum near-infrared (NIR) value to minimize the influence of shadows and understory (canopy openings between rows), as applied in Zarco-Tejada *et al.* (2001). However, in our case a ROI could potentially contain sub-pixels of neighboring trees due to a combination of imperfect tree positioning, overlapping ROIs, and artifacts due to upsampling.

4. Results

4.1. Vegetation indices

The most obvious characteristic of plants affected by *Fe* deficiency is leaf chlorosis (Morales *et al.*, 1994). This statement was also statistically verified as shown in Figure 3. Results of the logistic regression technique per wavelength (Delalieux *et al.*, 2006) are illustrated here. Based on the fact that *c*-values above 0.8 represent significant discriminative performance between the two treatments (0g and 60g of Sequestrene), it was concluded that a lack of iron applications resulted in differences in the spectral domain between 500 nm and 700 nm.

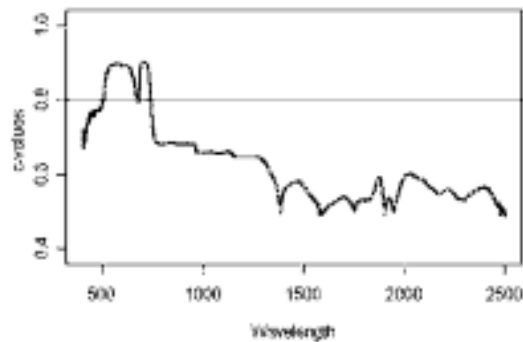


Figure 3: Discriminatory performance of the logistic regression per wavelength to discriminate between leaf spectra of iron treated (60g Sequestrene) and non-treated trees.

The investigation into vegetation indices corroborated these findings as shown below (Figure 4 and 5). Figure 4 represents the R^2 -values (>0.4) of a simple linear regression between all possible standardized vegetation indices $(\text{Wavelength 2} - \text{Wavelength 1}) / (\text{Wavelength 2} + \text{Wavelength 1})$ and measured chlorophyll concentrations.

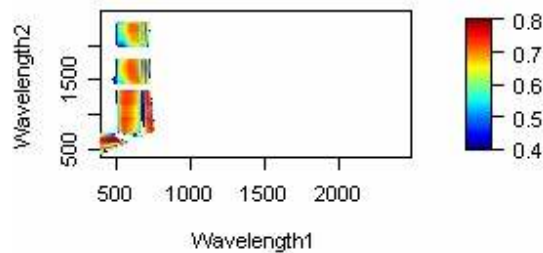


Figure 4: R^2 -values (>0.4) of a simple linear regression between all possible standardized vegetation indices and measured chlorophyll concentrations

The three dimensional graphs shown in Figure 5 represent the discriminatory performance (c -value) of logistic regression models at leaf (left), canopy (right) and airborne (black dots) level. The X- and Y-axes represent wavelength 1 and wavelength 2, respectively (see Eq.4), while the third dimension represents the c -index value visualized via color-coding. C -index values of 0.8 and more are indicative of good discrimination. All results are shown for leaf and canopy level, while for airborne level, due to the limited amount of wavelength bands, and thus also of results, only indices with c -values above 0.8 were plotted as black dots on top of the other images. Images (a) and (b) represent the discriminatory performance of the logistic regression model with as binary response variables: trees lacking any form of iron application (0) and trees treated with 60g of Sequestrene (1) at leaf and canopy level respectively. Logistic regression results for the trees treated with 60g and 120g are shown in figures (c) at leaf- and airborne level and in figure (d) at canopy- and airborne level. Finally, differences among trees treated with 90g and 120g of Sequestrene are illustrated in (e) and (f) at leaf and canopy level respectively. Since no black dots can be seen in the images (c-f), it can be concluded that iron deficiency is only detectable in extreme circumstances when using airborne imagery. This also counts for the research at leaf and canopy level where nearly no significant differences between trees with different iron applications could be found.

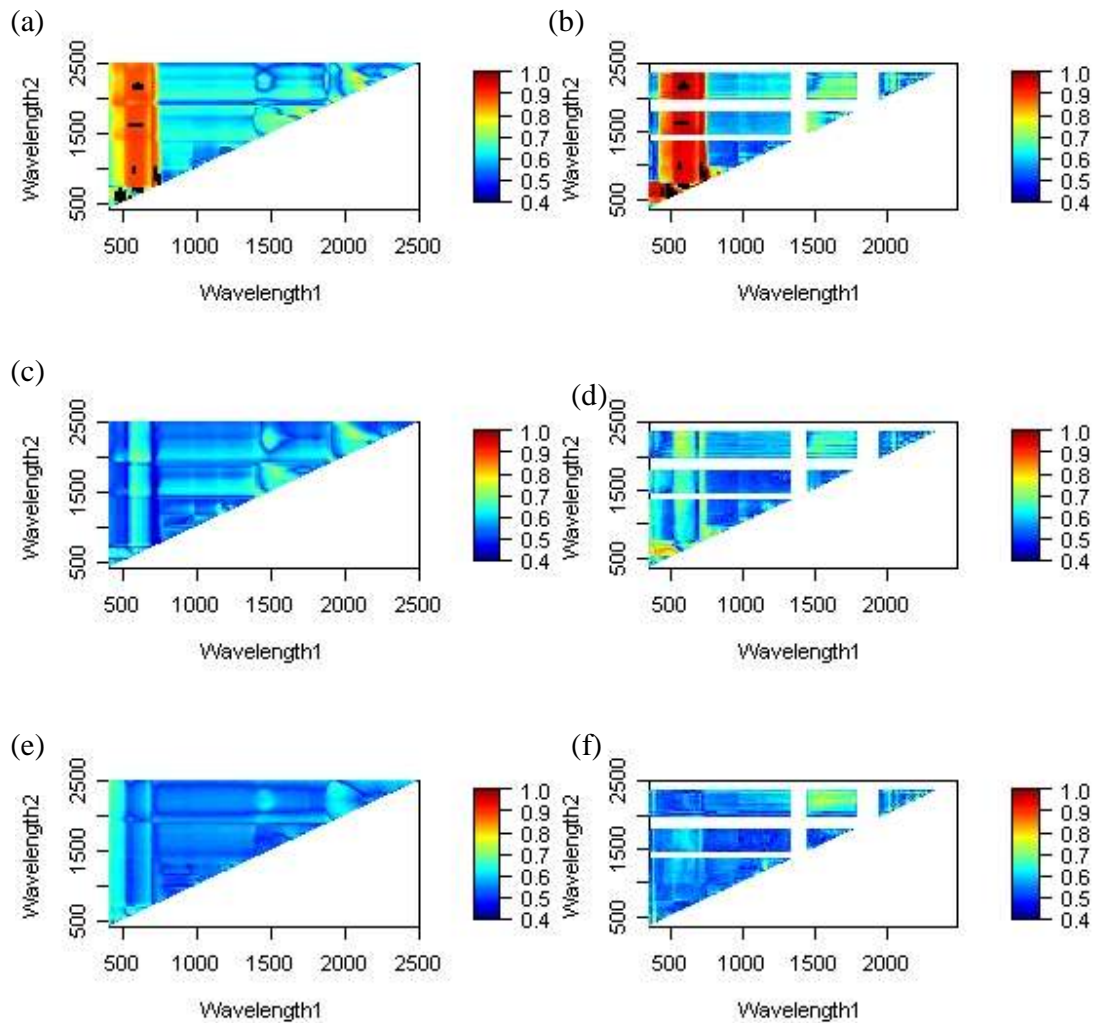


Figure 5 : Discriminatory performance (c-value) of logistic regression models with standardized vegetation indices as independent variables at leaf (left: (a),(c),(e)), canopy (right (b),(d),(e)) and airborne (black dots) level.

From Figures 4 and 5 it can be deduced that the most useful vegetation indices to detect iron stress are those that are closely related to chlorophyll concentration, which highlights the statement of iron deficiency causing chlorosis. Moreover, the combination of a chlorophyll sensitive band and an insensitive band holds more promise than a combination of two chlorophyll sensitive bands for the detection of iron stress. Out of the 63 AHS channels, channel 571 nm was selected as the most useful band when combined with a NIR (948 nm, 975 nm, 1004 nm) or SWIR (1622 nm, 2140 nm, 2152 nm, 2175 nm) channel for the extraction of the amount of chlorophyll or merely to discriminate between iron treated and iron untreated trees at leaf as well as at canopy and airborne levels. Vegetation indices based on only visible bands were not useful, probably due to the interaction of background and atmospheric effects. Schlerf *et al.* (2005) found that in forests a ratio index of wavelength 571 nm and 1622 nm was independent of the LAI. Hence, the combination of those wavelengths can be used very efficiently at leaf, TOC and airborne level. However, reflectance spectra are dominated by water absorption bands in NIR and SWIR regions leading to the supposition that the vegetative water content remained the same for all trees in this study.

4.2. Chlorophyll retrieval: regression at leaf level

Chlorophyll was estimated at the leaf level using different techniques. First, a predictive algorithm was derived from a simple regression technique using a single optimized band from the available ASD leaf spectra. A high correlation ($R^2=0.95$) and low RMSE of $1.78 \mu\text{g}/\text{cm}^2$ were obtained, indicating that chlorophyll in this particular instance can be derived accurately using even single-band leaf reflectance.

We have analyzed the importance of the spectral regions and bandwidths required by investigating the loss in predictive ability (correlation) if specific spectral regions were submitted. Figure 6 confirms that the visual part of the spectrum was most important for chlorophyll retrieval. The NIR was also able to predict chlorophyll concentrations, but correlation decreased as longer wavelengths (SWIR) were used. We also filtered the ASD input spectrum according to the AHS sensor specifications to verify whether the AHS sensor is suited to the task of chlorophyll retrieval. This is illustrated in Figure 7 where no degradation in correlation can be observed after filtering.

It furthermore was established that if the ASD spectra were further filtered, simulating multispectral sensors, good results were still obtained at the leaf level. It is useful to analyze the selected independent variable band after different filtering operations. As expected, for narrow bands with a full-width-at-half-maximum (FWHM) between 16nm and 32nm, the red-edge (702nm) provided valuable information on chlorophyll. However, the high frequency contained in the red-edge region will be discarded by a low pass filter and thus must be acquired with a narrow band. The selected band as a result moved towards the green peak (606nm) for increasing bandwidths. This is indicated in Figure 8, which shows the selected band as a shadowed region (with corresponding bandwidth). In the case where the leaf spectra were filtered according to the AHS sensor specifications, the fifth band (571nm) was selected. This was also the most appropriate band obtained in the logistic regression between different iron treatments. The cause-effect relationship between iron deficiency and chlorosis was once again emphasized.

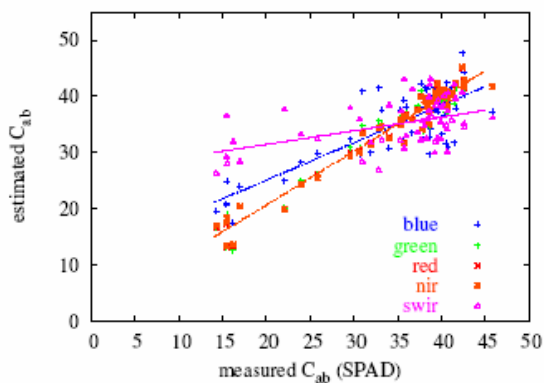


Figure 6: Simple linear regression for C_{ab} retrieval, submitting different parts of the spectrum.

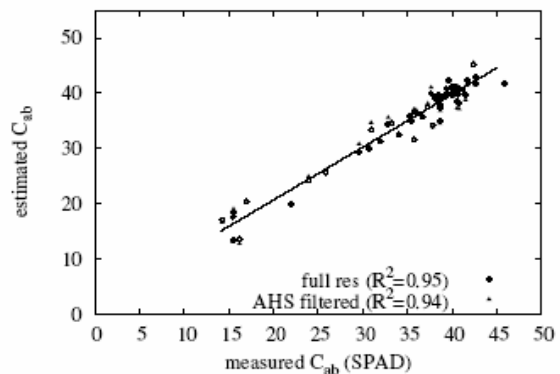


Figure 7: Simple linear regression for C_{ab} retrieval using the full ASD spectrum and a filtered spectrum according to the AHS sensor.

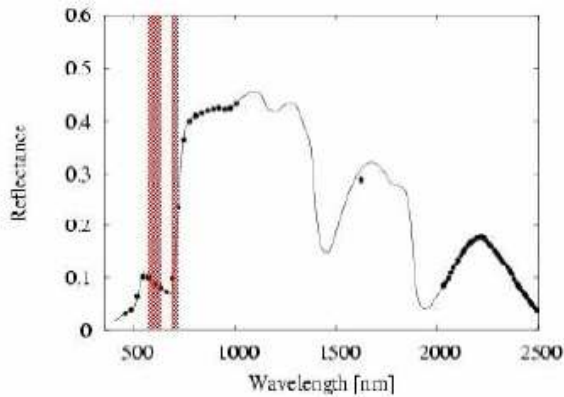


Figure 8: Selected bands for C_{ab} retrieval via simple linear regression. The red-edge is selected if high spectral resolution is available. For increasing bandwidths, the selected band is moved towards green peak.

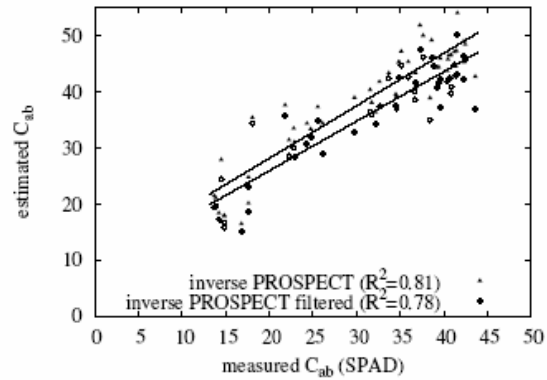


Figure 9: Chlorophyll estimation from leaf spectra through inversion of the PROSPECT leaf radiative transfer model. As for regression, filtering the spectra according to the AHS sensor specifications has only a slight impact on the result.

Despite the relatively good results of simple linear regression for chlorophyll retrieval, there are some drawbacks with this technique as mentioned in section 2. Inversion of radiative transfer models is an alternative that has been used with success (Jacquemoud *et al.*, 2000, Kuusk, 1998, Zarco-Tejada *et al.*, 2001).

Inversion of PROSPECT yielded good results for foliar chlorophyll retrieval (Figure 9, $R^2=0.81$, $RMSE=8.57 \mu g/cm^2$). Filtering the ASD spectra according to the AHS sensor specifications did not have a significant influence, thereby confirming the regression results. All five PROSPECT parameters were estimated by the optimization routine. Their mean values and variances are shown in Table 2.

Table 2: Means and variances of estimated PROSPECT parameters over all leaves

Parameter	Mean	Variance
Water equivalent thickness (C_w)	0.0121	9.9810^{-7}
Leaf protein content (C_p)	0.0002	1.810^{-20}
Leaf pigment concentration (C_c)	0.0031	1.0210^{-7}
Leaf structure parameter (N)	1.8	0.0047
Chlorophyll concentration (C_{ab})	39	98

It is clear from Table 2 that apart from chlorophyll, small variations in biochemical parameter values existed. As a result, those parameters were fixed at their mean value for further analysis at the canopy level.

4.3. Airborne hyperspectral data: canopy level

A total of 205 canopy spectra were derived from the AHS image as explained in section 3.3. A single spectrum was obtained for each tree by calculating the median reflectance for the corresponding region of interest.

The radiative transfer models PROSPECT and ACRM were inverted. C_{ab} was derived by first fixing the other four parameters for the PROSPECT leaf model at the mean values from Table 2. The canopy model parameters were fixed as well. The sun and view angles were set to the actual viewing geometry during the flight. The leaf area index (LAI) was measured for 10 trees with the LAI-2000 instrument. The mean value (1.71) was used as LAI input to the canopy model. The remaining parameters were fixed to the average value of the model range, or obtained by trial and error. This was the case for the leaf angle distribution (LAD) parameters, clumping and the refractive index of leaf scattering layers. The chlorophyll was not constrained. An overview of the fixed parameters for the canopy reflectance model is given in Table 3.

Table 3: Parameters used for the ACRM canopy reflectance model

Parameter	Value
Solar zenith angle	30°
Solar azimuth angle	121°
Relative viewing azimuth	0°
Angstrom turbidity factor	0.1
Leaf area index (LAI)	1.71
Leaf size	0.03
Clumping parameter	0.8
Log eccentricity term for LAD	2.3
Mean leaf angle of elliptical LAD	45
Refractive index of leaf scattering layers	1

A simple linear regression, similar to the chlorophyll retrieval from leaf reflectance, was performed for canopy level estimation. The regression performed best, followed by the proposed model inversion ($R^2=0.60$ and $RMSE=4.60\mu\text{g}/\text{cm}^2$ and $R^2=0.49$ and $RMSE=4.49\mu\text{g}/\text{cm}^2$, respectively). Figures 10 and 11 show the results for these two respective approaches. Appropriate filtering of the modelled reflectance and an improved optimization schedule increased the performance of model inversion considerably. E.g., standard model inversion using the conjugate direction method of Powell (Powell, 1964) for optimization underestimated higher chlorophyll concentrations ($R^2=0.34$ and $RMSE=10.59\mu\text{g}/\text{cm}^2$). Correlation of the Haboudane chlorophyll index, on the other hand, was an improvement over the standard model inversion ($R^2=0.41$), but underestimated the chlorophyll concentration by 50%, with a high RMSE as a result ($22.56\mu\text{g}/\text{cm}^2$).

Results at the plot level are presented in Figure 13, and show a good correlation between the pixels. Rows with low nutrient treatment appear in light color with low chlorophyll concentration. Even more noticeable is the column next to the treated trees (third from right). Those trees were grafted during the previous year, with a loss of chlorophyll concentration as a result. The best results were obtained using the regression approach, but training was required. The proposed model inversion also performed well, and is generally applicable to other species and geographical locations.

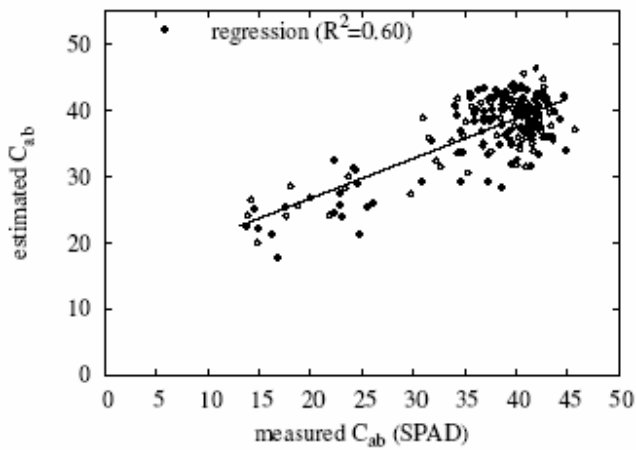


Figure 10: Chlorophyll estimation from hyperspectral image data using regression

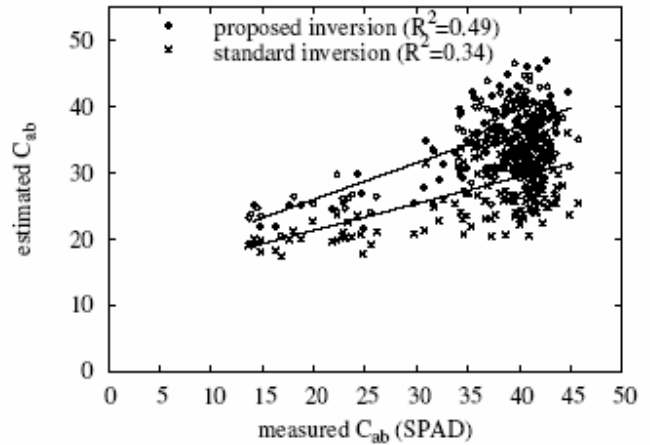


Figure 11: Chlorophyll estimation through model inversion using the proposed (filtering and adaptive simulated annealing) and standard methods (Powell, 1964).

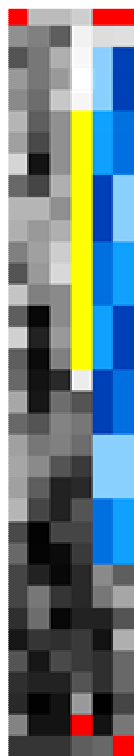


Figure 12: Schematic overview of the peach orchard. Treatment code (from light blue to dark blue): 0g/tree, 60g/tree, 90g/tree, and 120g/tree. The yellow pixels represent trees that have been grafted during the previous year.

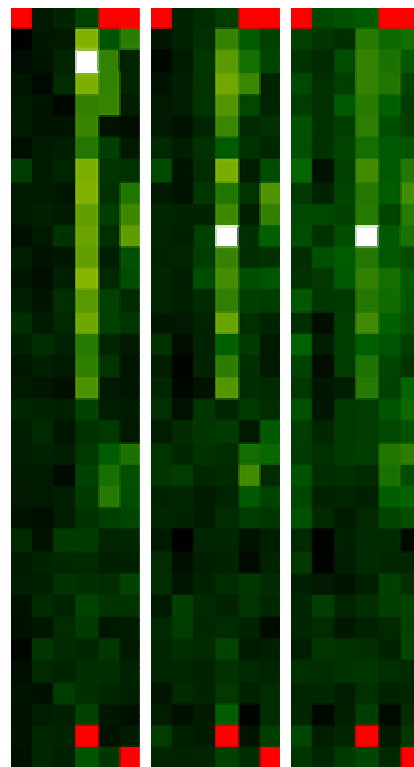


Figure 13: Chlorophyll content at the canopy level measured (left) and estimated using regression (middle) and model inversion (right). Chlorophyll concentration ranges from $13\mu\text{g}/\text{cm}^2$ (light green) to $46\mu\text{g}/\text{cm}^2$ (dark green).

5. Conclusions and further research

This study explored the potential of hyperspectral reflectance data to differentiate between iron deficient and healthy peach trees at leaf, canopy and airborne level. Logistic regression was used to identify wavelengths or wavelength domains that could differentiate among the different iron treatments within the peach orchard. Leaf chlorophyll concentration was estimated from *in situ* measured leaf reflectance and airborne hyperspectral imagery over a peach orchard. Although the variance of the chlorophyll estimation increased with the complexity of the two levels, the results showed that chlorophyll *a+b* content can be estimated from airborne hyperspectral data in a peach orchard for nutrient stress detection at the crown level. Model inversion of PROSPECT and ACRM also was successful, yielding leaf and canopy level values of $R^2=0.81$ and $R^2=0.49$ and $RMSE=8.57\mu g/cm^2$ and $RMSE = 5.49\mu g/cm^2$, respectively. However, special care must be taken for extraction of the canopy-level reflectance from the image data in order to minimize shadow and soil effects on the crown spectra.

Further research will focus on this issue of sample extraction and the assessment of a 3D model to take into account the bi-directional reflectance effects as function of the viewing geometry and scene components such as shadow and soil effects. Additional work is required for the validation of robust indices that allow efficient detection and quantification of anomalies in the normal plant production process at different observational scales. These indices easily can be incorporated in process models because of their numeric and compact character, thereby negating the need to collect full-range spectral datasets for monitoring vegetation production systems.

Our results suggested that early detection of abiotic plant stress using hyperspectral remote sensing has significant potential. This is of importance to the agricultural market, e.g., where an early warning system based on spectral inputs would be an ideal solution to the enforced reduction of pesticide or fertilization use. Farmers subsequently only have to apply these chemicals when and where biotic abnormalities are detected in the normal growth pattern of crops. Future at-satellite measurements will enable managers to obtain frequent hyperspectral coverage of large areas, thereby making continuous monitoring of biotic stress possible in capital-intensive crop production systems.

Acknowledgements

We would like to thank the Belgian Science Policy Office for financing this work. We also would like to acknowledge Drs. A. Kuusk and M. Disney for providing their code for the ACRM standard model inversion and Dr. L. Ingber for providing the ASA code.

References

- Blackmer, T. M., J. Schepers, G. Varvel, and E. Walter-Shea, "Nitrogen deficiency detection using reflected shortwave radiation from irrigated corn canopies." *Agronomy Journal* **88**, pp. 1-5, 1996.
- Camps-Valls, G., L. Bruzzone, J. L. Rojo-Royo, and F. Melgani, "Robust support vector regression for biophysical variable estimation from remotely sensed images." *IEEE Geoscience and Remote Sensing Letters* **3**, pp. 339-343, 2006.
- Carter, G.A., "Responses of Leaf Spectral Reflectance to Plant Stress." *American Journal of Botany*, **80**, pp. 239-243, 1993.
- Carter, G. A., "Ratios of leaf reflectances in narrow wavebands as indicators of plant stress." *International Journal of Remote Sensing* **15**, pp. 697-703, 1994.
- Chappelle, E. W., M. Kim, and J. M. III, "Ratio analysis of reflectance spectra (rars): An algorithm for the remote estimation of the concentrations of chlorophyll a, chlorophyll b, and carotenoids in soybean leaves." *Remote Sensing of Environment* **39**, pp. 239-247, 1992.
- Cordeiro, A. M., E. Alcantara, and D. Barranco, *Iron nutrition in soils and plants*, "Differences in tolerance to iron deficiency among olive cultivar." pp. 197-200. Kluwer, Netherlands, 1995.
- Curran, P. J., "Remote sensing of foliar chemistry," *Remote Sensing of Environment* **30**, pp. 271-278, 1989.
- Curran, P. J., J. L. Dungan, B. A. Macler, S. E. Plummer, and D. L. Peterson, "Reflectance spectroscopy of fresh whole leaves for the estimation of chemical concentration." *Remote Sensing of Environment* **39**, pp. 153-166, 1992.
- Daughtry, C. S. T., C. L. Walthall, M. S. Kim, E. B. de Colstoun, and J. E. McMurtrey, "Estimating corn leaf chlorophyll status from leaf and canopy reflectance." *Remote Sensing of Environment* **74**, pp. 229-239, 2000.
- Delalieux, S., J. van Aardt, W. Keulemans, E. Schrevels, I. Jonckheere, and P. Coppin. "Detection of biotic stress (*Venturia inaequalis*) in apple trees using hyperspectral data: Non-parametric statistical approaches and physiological implications." *European Journal of Agronomy*. Under review.
- Eitel, J.U.H., P.E. Gessler, A.M.S. Smith, and R. Robberecht. "Suitability of existing and novel spectral indices to remotely detect water stress in *Populus* spp." *Forest Ecology and Management* **229**, pp. 170-182, 2006.
- Filella I, L. Serrano, J. Serra, and J. Peñuelas. "Evaluating wheat nitrogen status with canopy reflectance indices and discriminant analysis." *Crop Science* **35**, pp. 1400-1405, 1995.
- Gamon, J., A. J. Penueles, and C. B. Field, "A narrow-waveband spectral index that tracks diurnal changes in photosynthetic efficiency." *Remote Sensing of Environment* **41**, pp. 35-44, 1992.
- Gamon, J.A., C.B. Field, M.L. Golden, K.L. Griffin, A.E. Hartley, G. Joel, J. Penueles, and R. Valentini, "Relationships between NDVI, canopy structure, and photosynthesis in three California vegetation types." *Ecological Applications*, **5**, pp. 28-41, 1995.
- Gitelson A. a., and M. N. Merzlyak, "Signature analysis of leaf reflectance spectra: Algorithm development for remote sensing of chlorophyll." *Journal of Plant Physiology* **148**, pp. 494-500, 1996.

Grossman, Y. L., S. L. Ustin, S. Jacquemoud, E. W. Sanderson, G. Schmuck, and J. Verdebout, "Critique of stepwise multiple linear regression for the extraction of leaf biochemistry information from leaf reflectance data." *Remote Sensing of Environment* **56**, pp. 1-12, 1996.

Haboudane, D., J.R. Miller, N. Tremblay, P.J. Zarco-Tejada, and L. Dextraze, "Integration of hyperspectral vegetation indices for prediction of crop chlorophyll content for application to precision agriculture." *Remote Sensing of Environment* **81**, pp. 416-426, 2002.

Ingber, L. "Adaptive simulated annealing (asa)." Lester Ingber Papers 93asa, Lester Ingber, undated. available at <http://ideas.repec.org/p/lei/ingber/93asa.html>.

Jacquemoud, S., "Inversion of the PROSPECT + SAIL canopy reflectance model from AVIRIS equivalent spectra: Theoretical study" *Remote Sensing of Environment* **44**, pp. 281-292, 1993.

Jacquemoud, S., F. Baret, B. Andrieu, F.M. Dansron, and K. Jaggard, "Extraction of vegetation biophysical parameters by inversion of the prospect + sail models on sugar beet canopy reflectance data. application to tm and aviris sensors." *Remote Sensing of Environment* **52**, pp. 163-172, 1995.

Jacquemoud, S., S. L. Ustin, J. Verdebout, G. Schmuck, G. Andreoli, and B. Hosgood, "Estimating leaf biochemistry using the PROSPECT leaf optical properties model." *Remote Sensing of Environment* **56**, pp. 194-202, 1996.

Jacquemoud, S., C. Bacour, H. Poilvé, and J. P. Frangi, "Comparison of four radiative transfer models to simulate plant canopies reflectance: direct and inverse mode," *Remote Sensing of Environment* **74**, pp. 471-481, 2000.

Kirkpatrick, S., C. D. J. Gerlatt, and M. P. Vecchi, "Optimization by simulated annealing," *Science* **220**, pp. 671-680, 1983.

Kokaly, R. F., and R. N. Clark, "Spectroscopic determination of leaf biochemistry using band-depth analysis of absorption features and stepwise linear regression." *Remote Sensing of Environment* **67**, pp. 267-287, 1999.

Kuusk, A. "A fast, invertible canopy reflectance model." *Remote Sensing of Environment* **51**, pp. 342-350, 1995.

Kuusk, A. "Markov chain model of canopy reflectance." *Agricultural Forest Meteorology* **76**, pp. 221-236, 1995.

Kuusk, A. "Monitoring of vegetation parameters on large areas by the inversion of a canopy reflectance model." *International Journal of Remote Sensing* **19**, pp. 2893-2905, 1998.

Kuusk, A. "Two-layer canopy reflectance model." on-line, August 2003.

Lichtenthaler, H. K. A. A. G. AA, and M. Lang, "Non-destructive determination of chlorophyll content of leaves of a green and an aurea mutant of tobacco by reflectance measurements." *Journal of Plant Physiology* **148**, pp. 483-493, 1996.

Lorenzen, B. and A. Jensen. "Changes in leaf spectral properties induced in barley by cereal powdery mildew." *Remote Sensing of Environment* **27**, 201-209, 1989.

Martin M. E., and J. D. Aber, "High spectral resolution remote sensing of forest canopy lignin, nitrogen and ecosystem process." *Ecological Applications* **7**, pp. 431-443, 1997.

Morales, F., A. Abadia, J. Abadia, "Iron deficiency-induced changes in the photosynthetic pigment composition of field-grown pear (*Pyrus communis* L.) leaves." *Plant, Cell and Environment* **17**, pp.1153-1160, 1994.

Moré, J.J. "The Levenberg-Marquardt Algorithm: Implementation and Theory," in G.A. Watson (ed.), *Lecture Notes in Mathematics 630*, Springer-Verlag, Berlin, pp. 105-116, 1978.

Nilson T. and A. Kuusk, "A reflectance model for the homogenous plant canopy and its inversion." *Remote Sensing of Environment* **27**, pp. 157-167, 1989.

Peñuelas, J., J. A. Gamon, A. L. Fredeen, J. Merino, and C. B. Field, "Reflectance indices associated with physiological changes in nitrogen- and water-limited sunflower leaves." *Remote Sensing of Environment* **48**, pp. 135-146, 1994.

Peñuelas J., I. Filella, J.A. Gamon, "Assessment of photosynthetic radiation-use efficiency with spectral reflectance at the leaf and canopy levels." In: Guyot G (Ed) Proceedings of the International Colloquium, *Photosynthesis and Remote Sensing*, 28-30 August, Montpellier, France, pp. 129-134, 1995.

Powell, M. J. D. "An efficient method for finding the minimum of a function of several variables without calculating derivatives." *Computer Journal* **7**, pp. 155 - 162, 1964.

Pu, R., S. Ge, N.M. Kelly, P. Gong, "Spectral absorption features as indicators of water status in coast live oak (*Quercus agrifolia*) leaves." *International Journal of Remote Sensing* **24**, pp.1799–1810, 2003.

Schlerf, M., C. Atzberger, J. Hill, "Remote sensing of forest biophysical variables using HyMap imaging spectrometer data." *Remote Sensing of Environment* **95**, pp. 177-194, 2005.

Tagliavini M., and A. D. Rombola, "Iron deficiency and chlorosis in orchard and vineyard ecosystems." *European Journal of Agronomy* **15**, pp. 71-92, 2001.

Wessman, C. A., J. D. Aber, D. L. Peterson, and J. M. Melillo, "Remote sensing of canopy chemistry and nitrogen cycling in temperate forest ecosystems." *Nature* **335**, pp. 154-156, 1988.

Zarco-Tejada, P. J., J. R. Miller, G. H. Mohammed, T. L. Noland, and P. H. Sampson, "Scaling-up and model inversion methods with narrow-band optical indices for chlorophyll content estimation in closed forest canopies with hyperspectral data." *IEEE Transactions on Geoscience and Remote Sensing* **39**, pp. 1491-1507, 2001.

Zarco-Tejada, P. J., J. R. Miller, A. Morales, A. Berjón, and J. Agüera, "Hyperspectral indices and model simulation for chlorophyll estimation in open-canopy tree crops." *Remote Sensing of Environment* **90**, pp. 463-476, 2004.